DOI: 10.1002/ange.201403096

Detecting H_2O_2 from Mitochondria

Electrochemical Monitoring of the Early Events of Hydrogen Peroxide Production by Mitochondria**

Emmanuel Suraniti, Salem Ben-Amor, Pauline Landry, Michel Rigoulet, Eric Fontaine, Serge Bottari, Anne Devin, Neso Sojic, Nicolas Mano, and Stéphane Arbault**

Abstract: *Mitochondria consume oxygen in the respiratory chain and convert redox energy into ATP. As a side process, they produce reactive oxygen species (ROS), whose physiological activities are still not understood. However, current analytical methods cannot be used to monitor mitochondrial ROS quantitatively and unambiguously. We have developed electrochemical biosensors based on peroxidase-redox polymer-modified electrodes, providing selective detection of H_2O_2 with nanomolar sensitivity, linear response over five concentration decades, and fast response time. The release of H_2O_2 by mitochondria was then monitored under phosphorylating or inhibited respiration conditions. We report the detection of two concomitant regimes of H_2O_2 release: large fluxes (hundreds of nM) under complex III inhibition, and bursts of a few nM immediately following mitochondria activation. These unprecedented bursts of H_2O_2 are assigned to the role of mitochondria as the hub of redox signaling in cells.*

The mitochondrion is a major organelle of aerobic cells, because it is the locus of energy production coupled to oxygen consumption. This process, namely oxidative phosphorylation, occurs at the inner membrane of the mitochondrion and involves complexes of the respiratory chain thermodynamically and kinetically coupled to ATP synthases.[1] It has been demonstrated that a major side process of the reduction of O_2 to water in the respiratory chain is the formation of reactive oxygen species (ROS, that is, at least $O_2^{\bullet-}$, H_2O_2, $OH^{\bullet}$). As a consequence, mitochondria possess an arsenal of strategies to scavenge these species and protect their own structures, including the mitochondrial DNA, against oxidative modifications. If the activities of superoxide dismutase (SOD), glutathione peroxidase (GPX), catalase (CAT), or thioredoxine (TRX) are decreased,[2] or under respiratory chain modulation,[3] mitochondria produce and release higher fluxes of ROS into the cytoplasm. These situations exert a general oxidative stress in the cell and also damage the mitochondria.

The oxidative metabolism of mitochondria is not fully understood. Recent literature shows that the mitochondrial ROS production is no longer considered an uncontrolled "desperate" situation solely leading to mitochondria or cell death.[2,4] Apparently, oxidative stress originating from mitochondria leads to severe pathological processes involved in genetic myopathies, neurodegenerative diseases including Alzheimer's disease (AD), and cancers.[5] However, it is also currently postulated that mitochondria produce ROS, and in particular H_2O_2, in a controlled manner to afford redox signaling within the cell (e.g. the activation of nuclear transcription factors)[6] and to control the mitochondrial population based on stimulated mitophagy.[7] The ROS production by mitochondria is usually analyzed using fluorescent dyes (e.g. MitoSox, Amplex Red, etc.). They enable the observation of processes within the cells even at the single-mitochondrion level.[8] Strikingly, bursts of superoxide, namely "superoxide flashes", were monitored within mitochondria and in their networks. They were recently hypothesized to be signatures of the redox signaling by and within mitochondria, and this heightens interest in their physiopathological role.[9]

However, fluorescent dyes suffer from analytical issues such as quenching and selectivity, which prevent a reliable quantification of the $O_2^{\bullet-}$ or H_2O_2 production by mitochondria.[10] In this respect, electrochemical sensors for ROS (at least $O_2^{\bullet-}$ and H_2O_2) have shown excellent analytical performances and great promise for biological applications.[11] Based on strategies of surface modification by catalysts like metallic particles, including platinum, and enzymes and surface structuration in 3D, a variety of electrodes with diameters in the mm to nm range have been reported.[12] They have been used for the detection of $O_2^{\bullet-}$ and H_2O_2 in tissues, on single cells, and even within a cell.[11a,13] However, they rarely have been applied to the detection of mitochondrial activity,[14] because of challenging analytical requirements. Indeed, the expected concentrations of released H_2O_2 account for only a fraction of the O_2 consumed by the

[*] S. Ben-Amor, Prof. N. Sojic, Dr. S. Arbault
Univ. Bordeaux, ISM, UMR 5255, Talence and
CNRS, ISM, UMR 5255, F-33405 Talence (France)
E-mail: stephane.arbault@u-bordeaux.fr
Dr. E. Suraniti, P. Landry, Dr. N. Mano
CNRS, CRPP, UPR 8641, Pessac and
Univ. Bordeaux, CRPP, UPR 8641, F-33600 Pessac (France)
E-mail: mano@crpp-bordeaux.cnrs.fr
Prof. M. Rigoulet, Dr. A. Devin
Univ. Bordeaux, IBGC, UMR 5095, Bordeaux and
CNRS, IBGC, UMR 5095, F-33077 Bordeaux (France)
Prof. E. Fontaine, Prof. S. Bottari
Université Grenoble-Alpes, Laboratory of Fundamental and Applied Bioenergetics, INSERM U1055, 38400 Saint Martin d'Hères (France)

[**] This project was financially supported by the ANR, project NANOMITO (no. ANR2011BSV502501), the Région Aquitaine (PhD fellowship for S.B.A.), Univ. Bordeaux and the CNRS (ATIP fellowship for S.A.).

Supporting information for this article including all details on both the preparation of biosensors and experiments on mitochondria is available on the WWW under http://dx.doi.org/10.1002/anie.201403096.

mitochondria, typically corresponding to a value in the wide nM–μM range. ROS production is a dynamic process, kinetically controlled by the conditions of mitochondrial activation or inhibition, which demands a fast response time of the sensor. Finally, selectivity may be an issue when nanomolar concentrations of H_2O_2 have to be accurately monitored in complex buffers. To overcome these issues, the goal of the present work is the design of such an ideal sensor and its use for the direct detection of a ROS, herein H_2O_2, produced and released by mitochondria under diverse conditions of activation, inhibition, and uncoupling.

We engineered an enzymatic biosensor with horseradish peroxidase (HRP), an enzyme that reduces H_2O_2 and has been widely used to develop electrochemical biosensors.[15] However, to our knowledge, previous devices never succeeded in reaching a very low detection limit (ca. 1 nM), while maintaining a linear response over several decades of H_2O_2 concentrations and a sufficiently fast response time. Our approach consists of embedding HRP in a cross-linked 3D polymer matrix bearing mobile osmium redox ($Os^{+/2+}$) mediators and permitting the diffusion of substrate.[16] Electrons, which reduce the analyte, are transferred from the electrode surface to the enzyme by step-by-step collisions of the redox mediators.

This method has achieved great success and its reliability has permitted widespread application for glucose sensing.[16,17] The ratio between the polymer, HRP, and the cross-linker must be properly chosen to optimize the electron transfer from the electrode to the polymer, through the polymer, then to HRP, and from HRP to H_2O_2 without affecting substrate diffusion. It is admitted in the literature that increasing the loading (i.e. the quantities of the enzyme, the redox polymer, and the cross-linker) on the electrode surface makes it possible to enhance the current density and therefore the detection limit. However, this is the case only in the absence of mass transport and/or kinetic limitations. Here, we have chosen the opposite strategy and decided to minimize the loading on the electrode surface.

Dotted lines in Figure 1 A represent the cyclic voltammograms (CVs) obtained with the modified electrodes for different loadings and are characteristic of a polymer-bound osmium complex with an apparent redox potential of +350 mV vs. Ag/AgCl. Upon addition of 1 mM H_2O_2, a clear reduction wave is observed, whose amplitude depends on the total loading (thick lines). The optimum ratio between components (HRP/polymer/cross-linker) was determined to be: 40 wt % deglycosylated HRP, 50 wt % PAA-PVI-[Os(4,4′-dichloro-2,2′-bipyridine)$_2$Cl]$^{+/2+}$, and 10 wt % poly(ethylene glycol) (400) diglycidyl ether. As previously demonstrated, deglycosylation enhances the electron transfer between the polymer and the enzyme and toughens the hydrogel.[18] The current densities of similar electrodes made without deglycosylation were a factor of 2 lower and less reproducible. Calibration curves measured at 0 V vs. Ag/AgCl are shown in Figure 1 B. For H_2O_2 concentrations of 1–100 μM, the current is independent of the loading, because the hydrogel is perfused with the substrate. For concentrations < 1 μM, the detection limit depends on the loading and therefore on the thickness of the film. For thin films (20 μg cm^{-2}), H_2O_2 is consumed in the entire hydrogel maximizing the electron transfer to the electrode surface. However, when the loading is ≥ 50 μg cm^{-2}, H_2O_2 is first reduced in the outer layer of the film, the mean distance for the electron transport to the electrode is increased, and the detection limit is thereby lowered. When the loading was < 20 μg cm^{-2}, no improvement of the detection limit was observed.

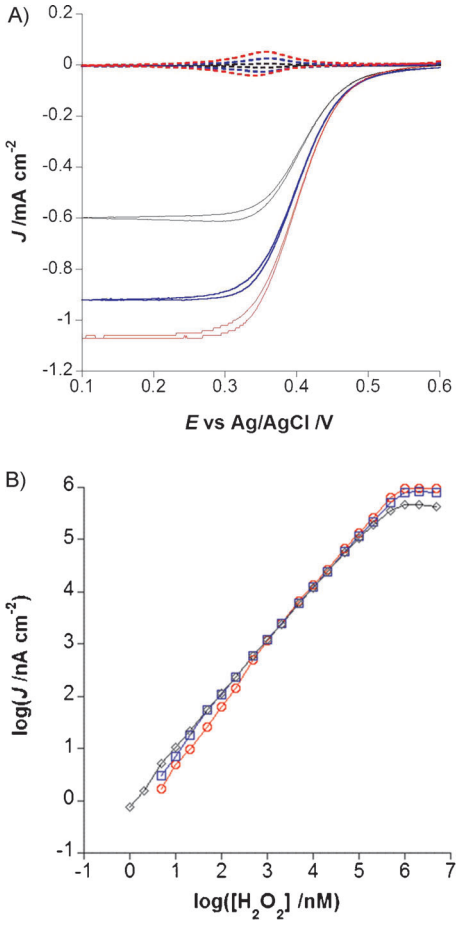

Figure 1. A) Cyclic voltammograms measured in the absence (dotted lines) and presence (solid lines) of 1 mM H_2O_2 for deglycosylated HRP electrodes with loadings of 100 (red line), 50 (blue line), and 20 μg cm^{-2} (black line) in a PBS buffer of pH 6.8 at 28 °C, 500 rpm, 5 mV s^{-1}. B) Resulting calibration curves measured at 0 V vs. Ag/AgCl (red: 100; blue: 50; black: 20 μg cm^{-2}).

Figure 2 shows an example of chrono-amperometric measurements on a modified HRP electrode with a loading of 20 μg cm^{-2}. H_2O_2 at a concentration of 1 nM was effectively detected (signal/noise ratio of 3), and the mean response time was 10 s. The standard deviation for ten measurements was ±4 %. By decreasing the loading of our hydrogel and using deglycosylated HRP, we succeeded in improving the detection limit and decreasing the response time. Our electrodes display the best sensitivity so far obtained for such a system (1.3 A M^{-1} cm^{-2}) in addition to excellent linearity over five orders of magnitude ($r^2 = 0.99$). These characteristics make the sensors ideal for real-time measurements of H_2O_2 released in vitro by mitochondria. Additionally, the electrode selectivity for H_2O_2 was determined during injections of

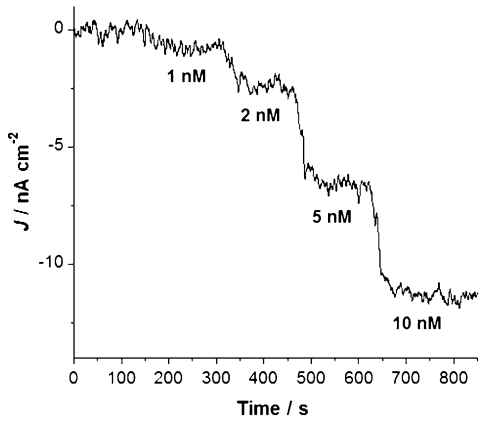

Figure 2. Chrono-amperometric detection at 0 V vs. Ag/AgCl of nanomolar H_2O_2 solutions. Loading: 20 μg cm^{-2}, conditions as described in Figure 1.

various substrates (ethanol, adenosine diphosphate) and an inhibitor (antimycin A) of the mitochondrial respiration. None of them induced a significant faradaic reaction of the biosensors, apart from current artifacts due to injection (Figure S1).

The release of H_2O_2 by mitochondria extracted from the yeast *Sacharomyces cerevisiae* was analyzed in an oxygraphy chamber equipped with both a Clark-type macroelectrode and the HRP biosensor, in an air-saturated buffer (see the Supporting Information for details) containing 1% ethanol. Ethanol was used as an energetic substrate, because it provides NADH to the respiratory chain upon conversion by alcohol dehydrogenase. Energized mitochondria rapidly decreased the local concentration of O_2 (negative slope of black curve in Figure 3) at a rate of 70 nmol min^{-1} mg^{-1}. ADP, the substrate of ATP synthases, was injected to gain a coupled oxidative phosphorylation state, thus increasing the rate of O_2 consumption by a factor of 1.9. Finally, antimycin A, an inhibitor of complex III of the respiratory chain, was injected,

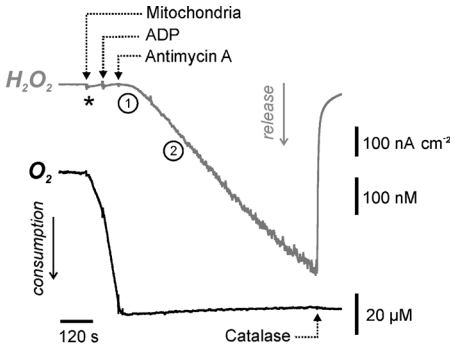

Figure 3. Chrono-amperometric monitoring of H_2O_2 production by mitochondria (gray curve, HRP electrode) and of their O_2 consumption (black curve, Clark macroelectrode at −850 mV vs. Ag/AgCl). Ethanol (1% final concentration) was injected to the aerated "respiratory" buffer (T = 28 °C) in the oxygraphy chamber prior to mitochondria (0.5 mg mL^{-1}), ADP (5 mM), and antimycin A (0.5 μM). The selectivity for H_2O_2 was confirmed by injecting exogenous catalase (400 u mL^{-1}). Two kinetic phases, labeled 1 and 2, have been identified for H_2O_2 release.

leading to the blockade of O_2 consumption. All these O_2 variations observed under conventional conditions were as expected (black curve).

Simultaneously, the H_2O_2 concentration (gray curve) in the solution was monitored: just following mitochondria addition, a spike-shaped signal of very low amplitude only lasting a few minutes was detected. After addition of ADP, no specific signal was observed. However, following addition of antimycin A, the reductive current started to increase in amplitude (i.e., more negative values) showing the in situ detection of H_2O_2 released by mitochondria. After a few minutes, the current linearly decreased corresponding to the accumulation of ca. 100 nM H_2O_2 min^{-1} mg^{-1} protein. The source of the signal was confirmed by addition of catalase to the medium, which rapidly and strongly diminished the HRP electrode signal (Figure 3). This first series of results demonstrated the ability of our biosensor to quantitatively monitor the H_2O_2 release during mitochondrial oxidative activities with an accuracy exceeding that reported with other methods (e.g. fluorescence).

In addition, the H_2O_2 curve in Figure 3 depicted some singular events. First, while O_2 consumption slowed down within 10 s after antimycin A addition, H_2O_2 was not released with a constant kinetic rate by mitochondria in the medium. One could identify two slopes in the current evolution corresponding to two regimes of H_2O_2 release, that is, within the first minute (regime 1: 15 μM min^{-1}), and thereafter (regime 2, see above). The delay in response could be attributed to a mitochondrial antioxidant activity aimed at controlling the H_2O_2 fluxes released. This hypothesis was confirmed by similarly measuring O_2 and H_2O_2 on mitochondria whose endogenous catalase activity was inhibited (see the Supporting Information for the procedure). Mitochondria treated with inhibitor released H_2O_2 at 15-fold higher rates (Figure S2) than untreated ones. Interestingly, there was almost no delay in H_2O_2 appearance in the medium, and no different kinetic regimes on curves for catalase-inhibited mitochondria were observed. This demonstrated the direct kinetic control of H_2O_2 efflux toward the external medium by catalase and possibly some other H_2O_2 scavengers located in the intermembrane space. Such observations may be ascribed to the mitochondrial control of H_2O_2 concentrations in ROS-dependent signaling processes.[9]

Initial spike-shaped signals (marked with * in Figure 3) were detected following either addition of mitochondria to a medium containing the energetic substrate (Figure 4A), or the addition of ethanol to the mitochondria, Figure 4B). In both cases, the spike-shaped signals appeared rapidly, reaching their maximum in less than 1 min and slowly decreasing toward the baseline within a few minutes. Owing to the extreme sensitivity of our sensor, we monitored local variations of at most 5 nM H_2O_2. Control experiments confirmed the origin of the signal: 1) no signal was detected in a medium deprived of O_2; 2) in a buffer supplemented with exogenous catalase only a short-term and low-amplitude artifact was detected, not corresponding to the H_2O_2 signal (Figure S1).

Consequently, we were able to identify two major modes of H_2O_2 release by mitochondria in these electrochemical

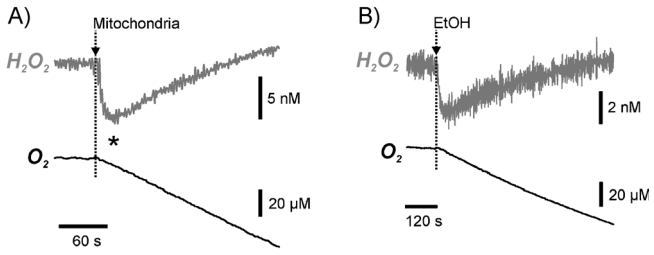

Figure 4. Chrono-amperometric monitoring of H_2O_2 release and O_2 consumption by mitochondria (conditions as described in Figure 3). A) Ethanol (1% concentration) was injected prior to mitochondria (0.5 mg mL^{-1}). B) Sequence opposite to that in A.

studies. The first one is detected under complex III inhibition, that is, at conditions aimed at transposing mitochondrial respiration towards ROS production. Our current results are based on a specific, quantitative, and kinetically resolved monitoring of H_2O_2, which cannot be obtained with any fluorescent dye (e.g. Amplex Red). This allows us to quantify the ratio of H_2O_2 release (linear part of the curve in Figure 3, state 3 inhibited) versus the O_2 consumption (at state 3 under oxidative phosphorylation coupling) as 0.5 to 1%. This value (often considered as a "leakage" of electrons from the O_2 reduction to H_2O) is in excellent agreement with values usually reported.[8b] Furthermore, we observed spikes of H_2O_2 release when mitochondria were temporally provided with ethanol. It is well known from fluorescent studies that this leads to an instant mitochondrial hyperpolarization, which might initiate superoxide production at the respiratory chain, and consequently leads to H_2O_2 formation and further release. Spike-type releases of superoxide by mitochondria, named superoxide flashes, were recently reported for several cell types.[19] They are increasingly considered to be a physiological response of mitochondria under calcium and membrane potential control. Herein, we measured unprecedented H_2O_2 burst-type releases of very similar duration to reported superoxide flashes. Because of the obvious coupling between H_2O_2 and $O_2^{\bullet-}$ production, we hypothesize that the two events are correlated. Meanwhile, in the present study, electrochemical biosensors could be used to measure the exact fluxes of H_2O_2 released by mitochondria, which might give a direct insight into their ROS-dependent signaling role in cells. To our knowledge, this has never been shown so far. Ultimately, these results should lead to further analytical developments to measure mitochondrial release of H_2O_2 within a cell or at the single-mitochondrion level to decipher the shift from physio- to pathological processes.

Received: March 7, 2014
Published online: May 22, 2014

Keywords: biosensors · horseradish peroxidase · hydrogen peroxide · mitochondria · redox signaling

[1] a) F. Scialo, V. Mallikarjun, R. Stefanatos, A. Sanz, *Antioxid. Redox Signaling* **2013**, *19*, 1953 – 1969; b) L. Galluzzi, O. Kepp, C. Trojel-Hansen, G. Kroemer, *Circ. Res.* **2012**, *111*, 1198 – 1207.
[2] P. Venditti, L. Di Stefano, S. Di Meo, *Mitochondrion* **2013**, *13*, 71 – 82.
[3] A. J. Kowaltowski, N. C. de Souza-Pinto, R. F. Castilho, A. E. Vercesi, *Free Radical Biol. Med.* **2009**, *47*, 333 – 343.
[4] a) L. Galluzzi, O. Kepp, G. Kroemer, *Nat. Rev. Mol. Cell Biol.* **2012**, *13*, 780 – 788; b) R. J. Mailloux, S. L. McBride, M. E. Harper, *Trends Biochem. Sci.* **2013**, *38*, 592 – 602.
[5] a) D. C. Wallace, *Nat. Rev. Cancer* **2012**, *12*, 685 – 698; b) S. Bolisetty, E. A. Jaimes, *Int. J. Mol. Sci.* **2013**, *14*, 6306 – 6344; c) D. Krstic, I. Knuesel, *Nat. Rev. Neurol.* **2013**, *9*, 25 – 34.
[6] C. Chevtzoff, E. D. Yoboue, A. Galinier, L. Casteilla, B. Daignan-Fornier, M. Rigoulet, A. Devin, *J. Biol. Chem.* **2010**, *285*, 1733 – 1742.
[7] R. J. Youle, A. M. van der Bliek, *Science* **2012**, *337*, 1062 – 1065.
[8] a) X. Q. Chen, X. Z. Tian, I. Shin, J. Yoon, *Chem. Soc. Rev.* **2011**, *40*, 4783 – 4804; b) S. I. Dikalov, D. G. Harrison, *Antioxid. Redox Signaling* **2014**, *20*, 372 – 382.
[9] a) W. Wang, H. Q. Fang, L. Groom, A. W. Cheng, W. R. Zhang, J. Liu, X. H. Wang, K. T. Li, P. D. Han, M. Zheng, J. H. Yin, W. D. Wang, M. P. Mattson, J. P. Y. Kao, E. G. Lakatta, S. S. Sheu, K. F. Ouyang, J. Chen, R. T. Dirksen, H. P. Cheng, *Cell* **2008**, *134*, 279 – 290; b) R. Mittler, S. Vanderauwera, N. Suzuki, G. Miller, V. B. Tognetti, K. Vandepoele, M. Gollery, V. Shulaev, F. Van Breusegem, *Trends Plant Sci.* **2011**, *16*, 300 – 309.
[10] J. F. Woolley, J. Stanicka, T. G. Cotter, *Trends Biochem. Sci.* **2013**, *38*, 556 – 565.
[11] a) C. Amatore, S. Arbault, M. Guille, F. Lemaitre, *Chem. Rev.* **2008**, *108*, 2585 – 2621; b) D. W. Kimmel, G. LeBlanc, M. E. Meschievitz, D. E. Cliffel, *Anal. Chem.* **2012**, *84*, 685 – 707.
[12] a) W. Chen, S. Cai, Q. Q. Ren, W. Wen, Y. D. Zhao, *Analyst* **2012**, *137*, 49 – 58; b) S. H. Chen, R. Yuan, Y. Q. Chai, F. X. Hu, *Microchim. Acta* **2013**, *180*, 15 – 32; c) J. Clausmeyer, P. Actis, A. López Córdoba, Y. Korchev, W. Schuhmann, *Electrochem. Commun.* **2014**, *40*, 28 – 30.
[13] Y. X. Wang, J. M. Noel, J. Velmurugan, W. Nogala, M. V. Mirkin, C. Lu, M. G. Collignon, F. Lemaitre, C. Amatore, *Proc. Natl. Acad. Sci. USA* **2012**, *109*, 11534 – 11539.
[14] a) S. Ben-Amor, A. Devin, M. Rigoulet, N. Sojic, S. Arbault, *Electroanalysis* **2013**, *25*, 656 – 663; b) R. Marcu, S. Rapino, M. Trinei, G. Valenti, M. Marcaccio, P. G. Pelicci, F. Paolucci, M. Giorgio, *Bioelectrochemistry* **2012**, *85*, 21 – 28.
[15] a) M. G. Garguilo, N. Huynh, A. Proctor, A. C. Michael, *Anal. Chem.* **1993**, *65*, 523 – 528; b) B. Lu, E. I. Iwuoha, M. R. Smyth, R. Okennedy, *Anal. Chim. Acta* **1997**, *345*, 59 – 66; c) B. Lu, E. I. Iwuoha, M. R. Smyth, R. Okennedy, *Anal. Commun.* **1997**, *34*, 21 – 24; d) E. E. Ferapontova, *Electroanalysis* **2004**, *16*, 1101 – 1112; e) K. Y. Inoue, K. Ino, H. Shiku, S. Kasai, T. Yasukawa, F. Mizutani, T. Matsue, *Biosens. Bioelectron.* **2010**, *25*, 1723 – 1728.
[16] A. Heller, *Curr. Opin. Chem. Biol.* **2006**, *10*, 664 – 672.
[17] A. Heller, B. Feldman, *Chem. Rev.* **2008**, *108*, 2482 – 2505.
[18] a) O. Courjean, V. Flexer, A. Prevoteau, E. Suraniti, N. Mano, *ChemPhysChem* **2010**, *11*, 2795 – 2797; b) R. Ortiz, H. Matsumura, F. Tasca, K. Zahma, M. Samejima, K. Igarashi, R. Ludwig, L. Gorton, *Anal. Chem.* **2012**, *84*, 10315 – 10323.
[19] a) S. Pouvreau, *PLoS One* **2010**, *5*, e13035; b) M. Schwarzländer, M. P. Murphy, M. R. Duchen, D. C. Logan, M. D. Fricker, A. P. Halestrap, F. L. Muller, R. Rizzuto, T. P. Dick, A. J. Meyer, L. J. Sweetlove, *Trends Cell Biol.* **2012**, *22*, 503 – 508; c) L. Wei, R. T. Dirksen, *J. Gen. Physiol.* **2012**, *139*, 425 – 434.